

Bismuth Amides as promising ALD Precursors for Bi₂Te₃ Films

Monika Rusek, T. Komossa, Georg Bendt, Stephan Schulz*

Institute of Inorganic Chemistry and Center for Nanointegration Duisburg-Essen (CENIDE), University of Duisburg-Essen, Universitätsstr. 5-7, D-45117 Essen, Germany. Fax: 44 0201 1833830; Tel: 44 0201 1834635; E-mail: stephan.schulz@uni-due.de

Abstract. The thermal properties of five homoleptic bismuth amides of the general type (R¹R²N)₃Bi (R¹, R² = Me **1**, R¹, R² = Et **2**, R¹, R² = *n*-Pr **3**, R¹ = Me, R² = Et **4**, R¹ = *n*-Bu, R² = Et **5**) and the cyclo-dibismadiazane [(Me₃Si)₂NBi- μ -NSiMe₃]₂ **6** were studied by DSC and TGA/DTA (**1**, **6**) and their reactions with (Et₃Si)₂Te were investigated by *in situ* NMR spectroscopy. Based on these results, the potential application of **1**, **4** and **6** to serve as ALD precursors for the deposition of Bi₂Te₃ films in reactions with (Et₃Si)₂Te were investigated. The resulting films were characterized by XRD, EDX, AFM and SEM and the crucial role of the substrate material and substrate temperature on the film growth rate and the morphology and chemical composition of the Bi₂Te₃ films was determined.

Keywords: A3. Atomic layer epitaxy; B1. Bismuth compounds; B1. Tellurites; B2. Semiconducting materials



This work may be used under a Creative Commons Attribution - NonCommercial - NoDerivatives 4.0 License (CC BY-NC-ND 4.0)

Introduction

The technical application of bismuth telluride, Bi_2Te_3 and antimony telluride, Sb_2Te_3 , in thermoelectric device applications and in photo optic applications thermoelectric devices has been studied for decades.^[1] The efficiency of a thermoelectric material is given by the dimensionless figure of merit ($ZT = (\alpha^2\sigma/\lambda)T$), where α is the Seebeck coefficient, σ is the specific electrical conductivity, λ is the thermal conductivity as sum of the electronic λ_{e1} and the lattice λ_{la} contribution and T the absolute temperature in Kelvin. Nanomaterials such as nanoparticles and thin films are promising candidates for thermoelectric applications since the thermal conductivity is often reduced compared to the bulk form due to increased phonon scattering at grain boundaries.^[2] For technical applications near room temperature, binary Bi_2Te_3 as well as ternary $(\text{Sb}_x\text{Bi}_{1-x})_2\text{Te}_3$ and quaternary $(\text{Sb}_x\text{Bi}_{1-x})_2(\text{Se}_y\text{Te}_{3-y})$ phases containing the heaviest elements of both groups are the most effective materials due to their high effective masses, high electrical conductivity, high Seebeck coefficient and glass-like low thermal conductivity.^[3] In addition, Bi_2Te_3 has received growing interest due to its promising application as topological insulator (TI),^[4] which are insulating materials in their bulk which form metallic conducting states on their surface due to strong spin-orbit coupling of the heavy elements.^[5] As a consequence, many researchers are interested in the synthesis of nanostructured Bi_2Te_3 nanoparticles as well as thin films with improved physical properties. Bi_2Te_3 nanoparticles are typically synthesized in wet chemical approaches by reaction of suitable Bi precursors such as bismuth acetate, bismuth oleate, bismuth nitrate, BiCl_3 or BiOCIO_4 with trioctyltellurophosphorane TOPTe or $(\text{Me}_3\text{Si})_2\text{Te}$.^[6] Recently, we reported on the low-temperature (< 120 °C) synthesis of different bismuth telluride phases including BiTe , Bi_2Te_3 and Bi_4Te_3 by thermal decomposition of the *single source precursor* Et_2BiTeEt or by reaction of bismuth triamides with bis(triethylsilyl)tellurane $(\text{Et}_3\text{Si})_2\text{Te}$ in diisopropylbenzene (DIPB)^[7a] as well as the synthesis of binary (Sb_2Te_3 , Bi_2Te_3) and ternary solid solutions $(\text{Bi}_x\text{Sb}_{1-x})_2\text{Te}_3$ by thermal decomposition of metal organic precursor in reactive ionic liquids.^[7b-d] Moreover, $(\text{Et}_3\text{Si})_2\text{Te}$ was also successfully applied in reactions with SbCl_3 and BiCl_3 for the deposition of Sb_2Te_3 and Bi_2Te_3 thin films by atomic layer deposition (ALD),^[8] while the analogous bis(triethylsilyl)selenane, $(\text{Et}_3\text{Si})_2\text{Se}$, was introduced as promising ALD precursor for the deposition of polycrystalline Bi_2Se_3 films by reaction with BiCl_3 .^[9] Unfortunately, the relatively high BiCl_3 source temperature, which is necessary due to the low vapor pressure of BiCl_3 , is a severe drawback since it limits the lowest deposition temperature usually to about 150 - 160 °C. These high deposition temperatures typically result in rather low growth rates. In addition, the use of metal halides such as BiCl_3 is often accompanied with corrosion problems due to the formation of HCl as well as the

incorporation of chlorine into the material film, which renders their use in ALD processes rather problematic. Therefore, alternative Bi ALD precursors with suitable vapor pressure and high reactivity are highly requested.

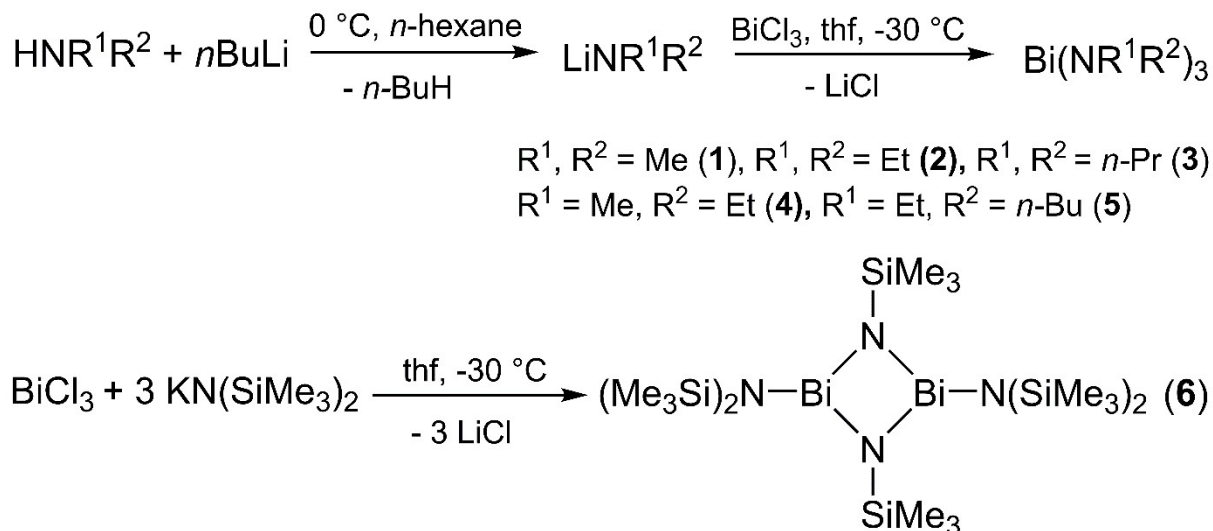
Bismuth triamides $(R_2N)_3Bi$ are promising ALD precursor candidates and $[(Me_3Si)_2N]_3Bi$ has been successfully applied for the ALD deposition of BiO_x films in reactions with water.^[10] In addition, $(Me_2N)_3Sb$ and $(Me_2N)_3Bi$ were previously applied for the wet chemical synthesis of Sb_2Te_3 and Bi_2Te_3 nanoparticles by reaction with $(Me_3Si)_2Te$ at very low temperature ($-30\text{ }^\circ\text{C}$) in organic solvents.^[11] These reactions were found to proceed with elimination of Me_3SiNMe_2 and appeared to be self-limiting, which is a pre-requisite for an ALD precursor. Moreover, $(Me_2N)_3Bi$ and $(Me_3Si)_2Te$ were used for the low-temperature deposition of Bi_2Te_3 films by *metal organic chemical vapor deposition* (MOCVD) process.^[12] However, the prerequisites for suitable ALD and CVD precursors fundamentally differ since thermal decomposition of the precursor is necessary in CVD processes while it is detrimental in ALD processes, which make use of precise chemical reactions between the precursors in order to guarantee self-limiting growth characteristics.

Atomic layer deposition (ALD) is a promising gas phase process for thin films deposition and in particular metal oxides have been investigated intensely over the last two decades.^[13] The film growth is self-limiting as long as no thermal decomposition of the precursors occurs and the thickness of the films can easily be controlled. The ideal ALD precursor is liquid or gaseous at ambient temperature and as reactive as possible to guarantee fast growth rates, but at the same time thermal as stable as possible to avoid thermal decomposition reactions. Since the wet chemical synthesis and the ALD process are both based on a specific chemical reaction between the precursors, bismuth triamides are promising ALD precursors since they were already applied in solution based synthesis of Bi_2Te_3 nanoparticles.^[7a,10,11] We became therefore interested in their use as ALD precursors and report herein on the thermal properties of five homoleptic bismuth amides $Bi(NR^1R^2)_3$ and the cyclo-dibismadiazane $[(Me_3Si)_2NBi-\mu-NSiMe_3]_2$ and their reactivity toward $(Et_3Si)_2Te$. Based on these results, the three most promising precursors were used in ALD deposition studies and the role of substrate material and substrate temperature on the film growth process and the resulting film morphology and composition was investigated.

Results and discussion

Five bismuth triamides of the general type $(R^1R^2N)_3Bi$ ($R^1, R^2 = Me$ **1**, $R^1, R^2 = Et$ **2**, $R^1, R^2 = n\text{-Pr}$ **3**, $R^1 = Me, R^2 = Et$ **4**, $R^1 = n\text{-Bu}, R^2 = Et$ **5**) were prepared according to literature method in almost quantitative yield by reaction of R^1R^2NLi with $BiCl_3$.^[14] In addition, the reaction of $KN(SiMe_3)_2$ with $BiCl_3$ yielded the cyclo-dibismadiazane $[(Me_3Si)_2NBi-\mu-$

NSiMe₃]₂ **6**, which was obtained as a product mixture with roughly 5% (Me₃Si)₃Bi as minor product as was reported by Evans et al.^[15] Recently, the synthesis and solid state structures of the comparable cyclo-dibismadiazanes [RN(SiMe₃)Bi- μ -NR]₂ (R = 4-Me-C₆H₄, 2,6-Me₂-C₆H₃) were reported.^[16]



Scheme 1. Synthesis of bismuth amides **1** - **6**.

The thermal properties of **1** - **6** were studied by differential scanning calorimetry (DSC) in a closed stainless steel screw cup under Ar atmosphere with a heating rate of 1 K per minute (Fig. S1). **1** to **5** decompose between 120 – 150 °C, while **6** shows a higher thermal stability ($T_{\text{onset}} = 258$ °C). According to these studies, (Me₂N)₃Bi **1**, (MeEtN)₃Bi **4** and [(Me₃Si)₂NBi- μ -NSiMe₃]₂ **6**, which show the highest decomposition onset temperatures, are the most promising ALD precursors, while **2**, **3** and **5** are expected to show stronger tendencies toward CVD-like growth at elevated temperatures due to their limited thermal stability.

The thermal properties of **1** and **6** were also investigated by TGA/DTA (Fig. S2). According to these studies, **1** shows a constant mass loss up to 150 °C, whereas the mass stays constant above this temperature. This finding most likely points to a decomposition process at high temperature. **6** shows a constant mass loss up to 200 °C, again proving its increased thermal stability compared to **1**. However, higher temperatures again result in decomposition. Black solids were obtained as residuals of both experiments.

The reactivity of the Bi precursors toward (Et₃Si)₂Te was further studied by *in situ* ¹H NMR spectroscopy. Previous studies showed that **1** readily reacts with (R₃Si)₂Te (R = Me, Et) at ambient temperature with elimination of the expected silylamine Me₂NSiR₃.^[7a,12a] In contrast, (Et₂N)₃Bi **2** required significantly longer reactions times (>20 h), while (n-Pr₂N)₃Bi **3**, (MeEtN)₃Bi **4** and (n-BuEtN)₃Bi **5** completely failed to react at ambient temperature.^[7] These results clearly prove the crucial role of the organic substituents on the reactivity of the bismuth triamides. We exemplarily monitored the reaction of (Et₃Si)₂Te with (n-Pr₂N)₃Bi **3** at

different reaction temperatures by $^1\text{H-NMR}$ spectroscopy (Fig. S1). **3** only reacted with $(\text{Et}_3\text{Si})_2\text{Te}$ at elevated temperature ($95\text{ }^\circ\text{C}$) with elimination of $n\text{-Pr}_2\text{NSiEt}_3$ (**3**), clearly proving that bismuth triamides $\text{Bi}(\text{NR}^1\text{R}^2)_3$ become kinetically more stabilized and hence less reactive with increasing steric demand of the substituents (R^1 , R^2). In addition, no indication was found for a reaction between **6** and $(\text{Et}_3\text{Si})_2\text{Te}$ even at $95\text{ }^\circ\text{C}$ within 24 h, proving that **6** is less reactive compared to **1** - **5**. However, since the reaction of **6** with $(\text{Et}_3\text{Si})_2\text{Te}$ was found to slowly proceed at $150\text{ }^\circ\text{C}$ with formation of Bi_2Te_3 nanoparticles, **6** was considered as high-temperature ALD precursor.

1 and **6** are the most promising ALD precursors due to their high reactivity (**1**) and enhanced thermal stability (**6**), whereas **2**, **3**, **4** and **5** lack from their low thermal stability and their lower reactivity. According to these findings, a successful ALD growth using **2** - **5** is expected to require rather high substrate temperatures, which unfortunately force an unwanted CVD growth. However, we also included precursor **4** in our ALD deposition studies since it is a liquid precursor at ambient temperature with reasonable thermal stability and a high vapor pressure, whereas **1** is a crystalline solid.

Table 1. Film growth parameters (precursor, substrate, $T_{\text{substrate}}$, no. of cycles) and chemical composition of the films as determined by EDX.

Film No.	Bi precursor	Substrate	$T_{\text{substrate}}$ ($^\circ\text{C}$)	No. of cycles	Bi (at%)	Te (at%)
I	1	Si(100) ^[a]	$70\text{ }^\circ\text{C}$	10000	38.50	61.50
II	1	Si(100)	$120\text{ }^\circ\text{C}$	4000	40.30	59.70
III	4	Si(100)	$120\text{ }^\circ\text{C}$	8500	39.04	60.96
IV	4	$\text{Al}_2\text{O}_3(0001)$	$120\text{ }^\circ\text{C}$	7000	40.39	59.61
V	4	Sb_2Te_3	$120\text{ }^\circ\text{C}$	4000	39.63	60.37
VI	6	Si(100)	$120\text{ }^\circ\text{C}$	4000	39.85	60.15
VII	6	SiO_2 ^[b]	$120\text{ }^\circ\text{C}$	4000	39.33	60.67
VIII	6	Si(100)	$170\text{ }^\circ\text{C}$	4000	39.15	60.85
IX	6	SiO_2	$170\text{ }^\circ\text{C}$	100	40.89	59.11
X	6	SiO_2	$170\text{ }^\circ\text{C}$	500	40.36	59.64
XI	6	SiO_2	$170\text{ }^\circ\text{C}$	1000	40.64	59.36
XII	6	SiO_2	$170\text{ }^\circ\text{C}$	4000	40.89	59.11

^[a] Si(100) substrates with a native SiO_2 layer; ^[b] SiO_2 substrates with a 500 nm thick SiO_2

layer; the bubbler temperature for $(\text{Et}_3\text{Si})_2\text{Te}$, **1** and **4** were kept constant at 25 °C, while the bubbler with precursor **6** was heated to 100 °C.

ALD deposition studies were performed in a home-made ALD reactor and the deposition parameters such as substrate material and substrate temperature, which are summarized in Table 1, were varied in order to investigate their influence on the resulting film composition and film morphology. The $(\text{Et}_3\text{Si})_2\text{Te}$ pulse length, which is the time for which the source valve is opened, was kept constant at 0.2 - the accessible flow minimum in our home-made reactor system - due to the high volatility of the Te precursor, while the $\text{Bi}(\text{NR}^1\text{R}^2)_3$ pulse was fixed to 0.4 sec due to the lower vapor pressure of the bismuth precursors. After the precursors are introduced into the ALD chamber, the source valve is closed and they are allowed to react at the surface (exposure modus) for different times ($t_{\text{exposure}} = 15, 20$ sec). The elemental composition of the resulting material films was determined by energy dispersive X-ray analysis (EDX). Almost ideal Bi/Te molar ratios of 40:60 were obtained for each film, proving the formation of pure Bi_2Te_3 films (Table 1)

The crystalline nature of each Bi_2Te_3 films was shown by grazing incidence X-ray diffraction (GIXRD). All Bragg reflexes with a significant intensity can be indexed on the basis of the structure of rhombohedral Bi_2Te_3 (JCPDS–ICDD 00-015-0863) as exemplarily shown for the film obtained with **1** at very low substrate temperature of only 70 °C (Fig. 1; additional X-ray diffractograms are given in the electronic supplement, Figs. S3-S5).

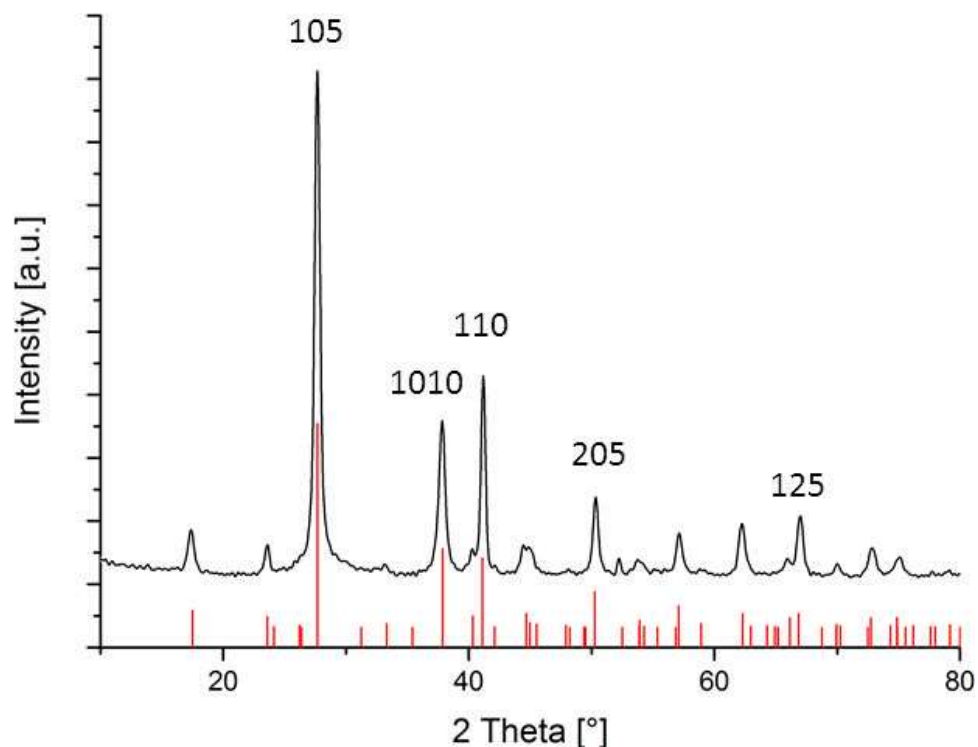


Figure 1. GIXRD pattern of a Bi_2Te_3 film (**I**) deposited on Si(100) at 70 °C with $(\text{Me}_2\text{N})_3\text{Bi}$ **1**; peaks of Bi_2Te_3 in red (JCPDS–ICDD 00-015-0863); only the reflections with highest intensity are marked.

The surface morphology of the Bi_2Te_3 films deposited at low-temperature (70 °C) on Si(100) using precursor **1** (**I**) as well as those deposited at higher temperature (120 °C) using precursors **4** (**III**) and **6** (**VI**) was investigated by SEM (Fig. 2). The formation of rather polycrystalline films consisting of hexagonal Bi_2Te_3 nanoplates, which are randomly oriented with respect to the substrate, is clearly visible in the SEM photographs. Obviously, the low substrate temperatures reduce the mobility of the adatoms on the substrate surface during film growth, which is necessary for the formation of a smooth film.

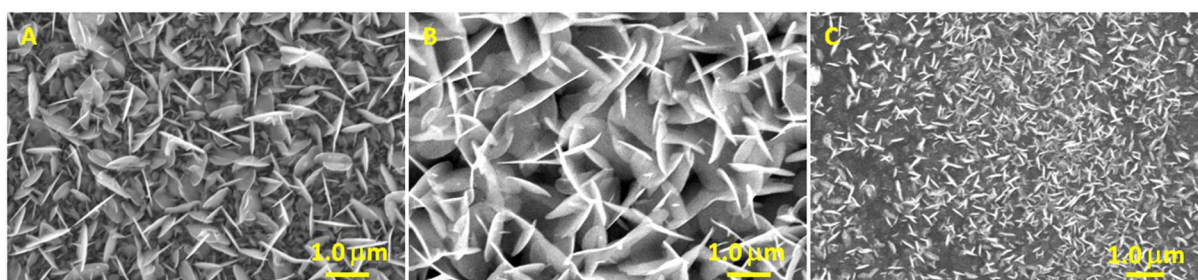


Figure 2. SEM pictures of Bi_2Te_3 films deposited with $(\text{Me}_2\text{N})_3\text{Bi}$ **1** (A, **I**), $(\text{MeEtN})_3\text{Bi}$ **4** (B, **III**) and $[(\text{Me}_3\text{Si})_2\text{NBi}-\mu\text{-NSiMe}_3]_2$ **6** (C, **VI**) on Si(100).^[17]

Polycrystalline Sb_2Te_3 and Bi_2Te_3 films have been previously obtained by ALD deposition, while flat Sb_2Te_3 films were formed on OH-terminated oxide interfaces of Si substrates,^[8h,18] clearly indicating a strong influence of the substrate material on the growth mechanism. In addition, Leskelä et al. reported on the ALD growth of Bi_2Te_3 films at a higher substrate temperature (160 °C) on SiO_2/Si substrates by reaction of BiCl_3 and $(\text{Et}_3\text{Si})_2\text{Te}$.^[8h] The film growth was monitored after several cycles, proving the initial formation of small grains, which became larger and finally coalesced to a smooth film with increasing number of deposition cycles, resulting in the formation of three-dimensional polycrystalline Bi_2Te_3 films consisting of flakes with sizes of several hundred nanometers. The authors claimed that the formation of polycrystalline films is an inherent property of Bi_2Te_3 , which may be attributed to its layered crystal structure. In addition, temperature dependant ALD deposition studies revealed the formation of smooth Bi_2Te_3 films in the temperature range between 160 and 200 °C. We therefore investigated the specific influence of the substrate material as well as the substrate temperature on the film growth and deposited Bi_2Te_3 on different substrates such as Si(100), $\text{Al}_2\text{O}_3(0001)$ and Sb_2Te_3 (Fig. 3).

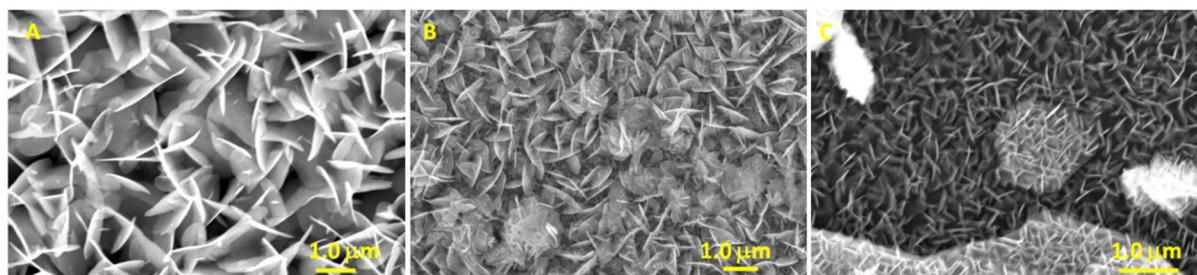


Figure 3. Typical surface morphologies of Bi_2Te_3 films deposited at 120 °C using $(\text{Et}_3\text{Si})_2\text{Te}$ and $(\text{MeEtN})_3\text{Bi}$ **4** on Si(100) (A, **III**), $\text{Al}_2\text{O}_3(0001)$ (B, **IV**) and on MOCVD-grown Sb_2Te_3 (C, **V**).^[19]

All ALD experiments using **1**, **4** and **6** yielded polycrystalline Bi_2Te_3 films with randomly oriented Bi_2Te_3 hexagonal plates as was verified by powder X-ray diffraction and SEM. According to these studies, the influence of the substrate material on the film morphology seems to be rather limited. However, we demonstrated in previous CVD studies that epitaxial Sb_2Te_3 and Bi_2Te_3 films were deposited on Al_2O_3 substrates at higher temperatures of about 400 °C,^[19] whereas the CVD deposition of a single source precursor $(\text{Et}_2\text{Sb})_2\text{Te}$ at low temperature (200 °C) only yielded polycrystalline Sb_2Te_3 films.^[20] Obviously, the substrate temperature plays a major role in CVD deposition and we think that this is also true for ALD processes. In order to prove the influence of the substrate temperature on the resulting film morphology, ALD deposition studies were performed at a higher substrate temperature (170 °C), which is in the optimal temperature range as reported by Leskelä et al. (160 - 200 °C).^[8h] **1** and **4** were excluded from these studies since they already start to decompose at lower temperatures (140 °C) as was demonstrated by DSC experiments and, as a consequence, CVD-like growth was expected to occur at high temperature. In contrast, $[(\text{Me}_3\text{Si})_2\text{NBi}-\mu\text{-NSiMe}_3]_2$ **6** is thermally stable up to almost 260 °C and we therefore investigated ALD film growth both on Si(100) and on SiO_2 substrates (Fig. 4).

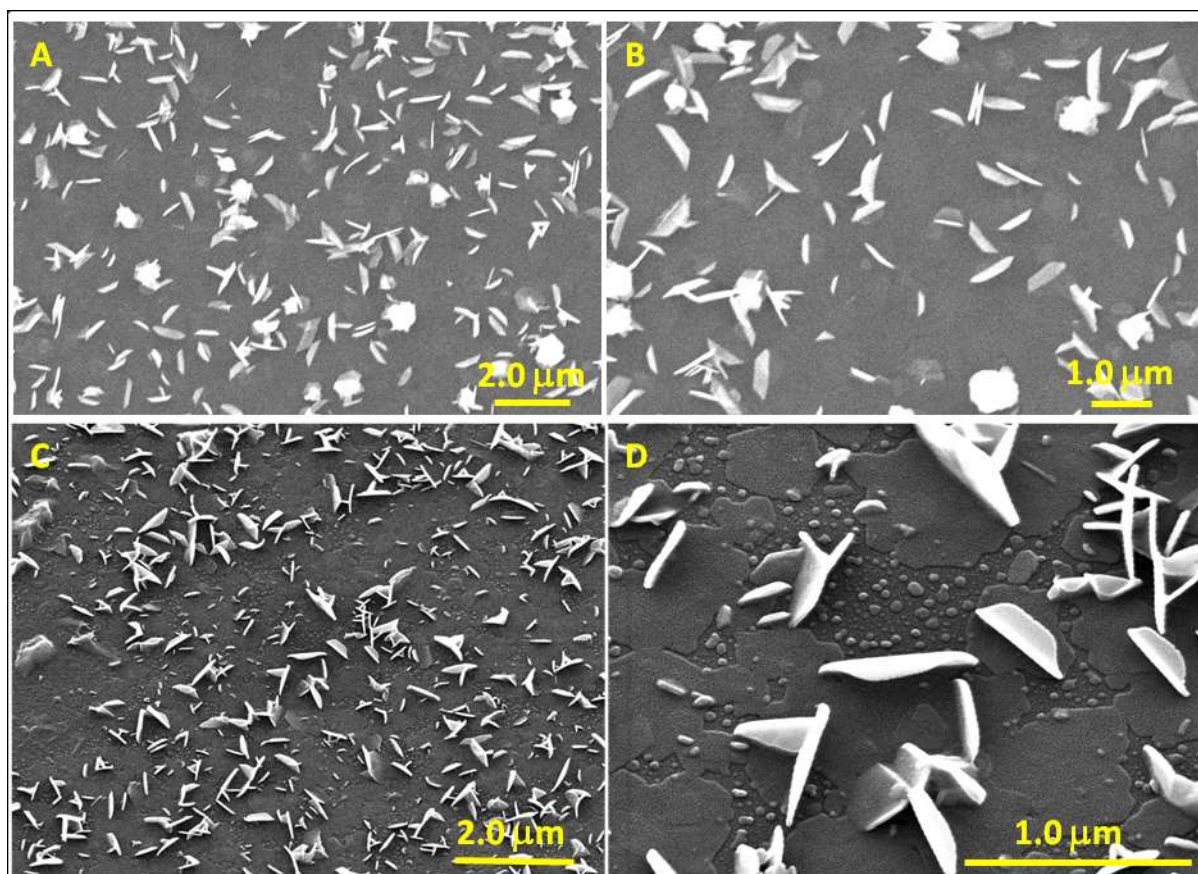


Figure 4. Surface morphology of Bi_2Te_3 films deposited with $(\text{Et}_3\text{Si})_2\text{Te}$ and $[(\text{Me}_3\text{Si})_2\text{NBi}-\mu\text{-NSiMe}_3]_2$ **6** at $170\text{ }^\circ\text{C}$ on $\text{Si}(100)$ (A, B **VIII**) and SiO_2 (C, D **X**).

SEM images clearly reveal the growth of smoother Bi_2Te_3 films on the substrate. However, additional perpendicular-oriented nanoplates are also visible, but the number of these nanoplates is lower compared to the films deposited at lower substrate temperatures. These results demonstrate the crucial influence of the substrate temperature on the resulting film morphology and the results agree with those reported by Leskelä et al. using BiCl_3 .^[8h] Obviously, the mobility of the adatoms on the substrate is reasonable higher at $170\text{ }^\circ\text{C}$ compared to $120\text{ }^\circ\text{C}$, resulting in the formation of smooth films. The number of perpendicular-oriented Bi_2Te_3 nanoplates does not significantly increase with increasing cycle number, hence their formation clearly depends on the substrate temperature (Fig. 5).

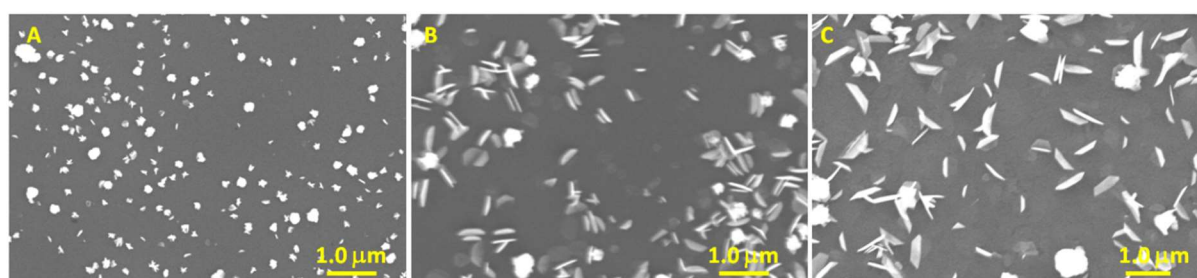


Figure 5. SEM images of Bi_2Te_3 films obtained with $(\text{Et}_3\text{Si})_2\text{Te}$ and $[(\text{Me}_3\text{Si})_2\text{NBi}-\mu\text{-NSiMe}_3]_2$ **6** at $170\text{ }^\circ\text{C}$ on a $\text{Si}(100)$ substrate containing a native oxide layer after 500 cycles (A, **X**), 1000 cycles (B, **XI**) and 4000 cycles (C, **XII**).

GIXRD patterns of Bi₂Te₃ films as obtained with precursor **6** at different temperatures were measured with a fixed angle of incidence of 1° (Fig. S5). All Bragg peaks with significant intensity can be indexed on the basis of the structure of rhombohedral Bi₂Te₃ (JCPDS–ICDD 00-015-0863) and no additional peaks were detected. The GIXRD pattern of the film deposited at 170 °C (Fig. S5A) doesn't show the (00l) reflections in higher intensity formation compared to those deposited at 120 °C (Fig. S5B) and 70 °C (Fig. 1), respectively. However, this is likely since the intensity of the reflections caused by the perpendicular-oriented crystallites is higher compared to those of the c-oriented crystallites on the surface in GIXRD experiments.

Table 2. Film thickness (FT) [nm] and growth rate per cycle (GRPC) [Å] of the Bi₂Te₃ films deposited with (Et₃Si)₂Te and [(Me₃Si)₂NBi-μ-NSiMe₃]₂ **6** at 170 °C on three different substrates as determined by AFM.

no. of cycles	Al ₂ O ₃		Si		SiO ₂	
	FT [nm]	GRPC [Å]	FT [nm]	GRPC [Å]	FT [nm]	GRPC [Å]
200	60	3.00	55	2.75	70	3.50
2000	156	0.78	233	1.16	250	1.25
4000	263	0.66	430	1.07	450	1.13

Since smooth Bi₂Te₃ films were obtained with precursor **6** at high substrate temperature (170 °C), we investigated the ALD process using **6** in more detail. ALD deposition processes using **6** were performed on three different substrates (Si100, SiO₂ and Al₂O₃) at 170 °C and the growth rates were determined by AFM by measuring the thickness of three Bi₂Te₃ films deposited with different number of cycles. For this purpose, the substrates were partly masked with a temperature stable cello tape, which was removed after deposition and the cantilever scanned in the line-scan mode over the edge (uncoated surface – coated surface). The line-scan was performed 15 - 25 times for each sample around and the given film thicknesses represent average values (table 2). Unfortunately, ALD deposition at higher substrate temperatures couldn't be investigated since 170 °C is the maximum substrate temperature that can be achieved with our ALD reactor.

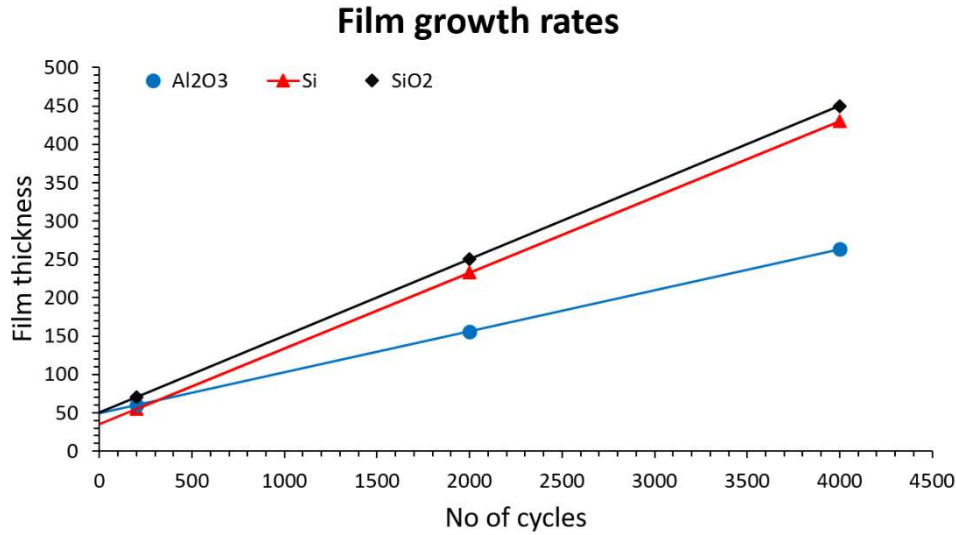


Figure 6. Diagram of the film thickness as a function of cycle numbers. The large change of the nominal growth rate vs. film thickness most likely results from a non-ideal 2D nucleation on the substrate.

Figure 7 shows the height profile of a Bi₂Te₃ film as-obtained after 2000 cycles on SiO₂. It illustrates the growth of Bi₂Te₃ flakes which results in a film roughness comparable to values previously reported.^[8h]

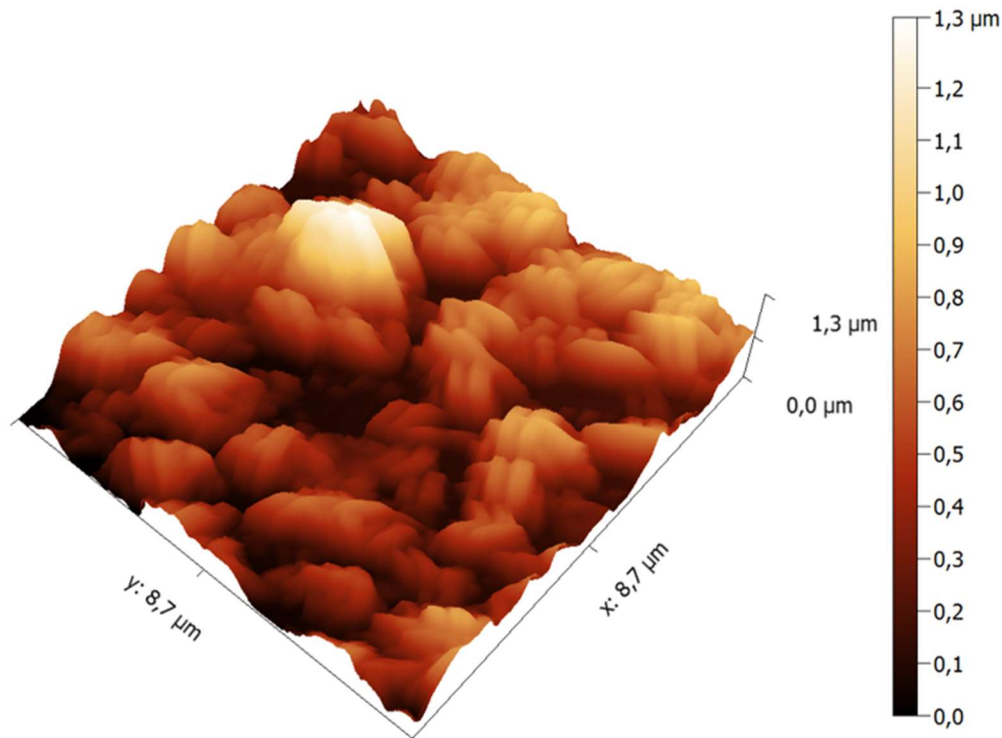


Figure 7. AFM image of a Bi₂Te₃ deposited on a SiO₂ substrate after 2000 cycles using 6.

The film growth rates on Si and SiO₂ substrates are comparable and significantly higher compared to that on Al₂O₃. The film growth is nearly linear for all substrates, but the graphs

don't go through the origin of the coordinate system (Fig. 6). These findings most likely result from the formation of orthogonally oriented Bi_2Te_3 crystallites even in the beginning of the deposition process, resulting in an overestimation of the film thickness and leading to unrealistic high growth rates in the early stage of the film growth process. After 1000 cycles, the growth rates become almost constant around 0.7 Å (Al_2O_3), 1.1 Å (Si) and 1.2 Å (SiO_2), respectively, indicating that the initially formed polycrystalline films change to a smoother film by filling the spaces between the Bi_2Te_3 -flakes.

Leskelä et al. reported on the ALD growth of Bi_2Te_3 films at different substrate temperatures between 160 and 250 °C.^[8h] Growth rates up to 1.1 Å/cycle were observed at 160 °C, while they were found to steadily decrease with increasing substrate temperature and no film was obtained at a temperature of 250 °C, which points to increasing precursor desorption with increasing substrate temperature.^[13c] Comparable findings have been previously reported for ALD film growth processes using alkylsilyl telluride precursors^[21] and this temperature dependency seems to be characteristic for ALD processes. Our findings presented herein fit very well to these studies.

Conclusions. Five homoleptic bismuth amides $(\text{R}^1\text{R}^2\text{N})_3\text{Bi}$ (**1** - **5**) and cyclo-dibismadiazane $[(\text{Me}_3\text{Si})_2\text{NBi}-\mu\text{-NSiMe}_3]_2$ **6** were investigated in respect to their use as ALD precursor in reactions with $(\text{Et}_3\text{Si})_2\text{Te}$. **1** - **5** showed a lower thermal stability compared to **6** as was confirmed by differential scanning calorimetry (DSC), while their reactivity toward $(\text{Et}_3\text{Si})_2\text{Te}$ is higher than that of **6**. The reactions proceeded with elimination of the expected silylamines as was confirmed by *in situ* $^1\text{H-NMR}$ spectroscopy. ALD studies were performed with three different Bi precursors (**1**, **4**, **6**) on different substrate temperatures and different substrate materials and the resulting films were characterized by XRD, EDX and SEM. Polycrystalline Bi_2Te_3 films were obtained at low substrate temperatures (120 °C), which is the maximum growth temperature for **1** and **4** due to their limited thermal stability. In contrast, $[(\text{Me}_3\text{Si})_2\text{NBi}-\mu\text{-NSiMe}_3]_2$ **6** shows a higher thermal stability, hence allowing higher substrate temperatures. ALD deposition studies at 170 °C on SiO_2 substrates resulted in the growth of smooth crystalline Bi_2Te_3 films. According to these studies, relatively high substrate temperatures are essential in order to obtain flat films, hence requiring the development of alternate, thermally stable bismuth precursors.

Acknowledgement. S. Schulz thanks the Deutsche Forschungsgemeinschaft (DFG) for financial support of this work within the priority program SPP 1666 (Topological Insulators).

Experimental Section

Materials: *N*-hexane and Et_2O were carefully dried using a solvent purification system (MBraun) and degassed prior to use. THF was dried by refluxing over Na/K alloy for several

days, distilled and degassed prior to use. 2.5 M *n*-BuLi solution in *n*-hexane, BiCl₃, Me₂NH, Et₂NH, *i*-Pr₂NH, MeEtN, *n*-BuEtNH and KN(SiMe₃)₂ were commercially available. The amines were stored over molecular sieves for several days and degassed prior to use.

(Et₃Si)₂Te,^[22] bismuth triamides (Me₂N)₃Bi **1**, (Et₂N)₃Bi **2**, (*n*-Pr₂N)₃Bi **3**, (EtMeN)₃Bi **4**, (*n*-BuEtN)₃Bi **5**^[14] and [(Me₃Si)₂NBi- μ -NSiMe₃]₂ **6**^[15] were synthesized according to slightly modified literature methods (SI). All synthetic steps were performed under argon atmosphere using standard Schlenk techniques or a glovebox.

ALD Reactor. ALD studies were performed in an ALD reactor which contains three precursor supplies (bubbler), through which argon gas is bubbled. The supplies are connected to electronic valves, which control the pulse times of the precursors streaming into the reaction chamber. The chamber can only be heated up to 200 °C.

ALD Deposition Parameters. The films were deposited onto 1 × 1 cm² substrates under a pressure of about 0.8 mbar using Ar as carrier and N₂ as purging gas. The Te precursor (Et₃Si)₂Te was evaporated from an open glass vessel at 25 °C and pulsed with inert gas.

Table 3. ALD deposition parameters as applied with precursors **1**, **4** and **6**.

(R ¹ R ² N) ₃ Bi	T _{precursor} [°C]	T _{valves} [°C]	T _{chamber} [°C]	t _{exposure} [s]	t _{pump} [s]
1	25	60	70, 120	15, 20	20, 25
4	25	60	120	15, 20	20, 25
6	100	110	120, 170	20	25

Characterization Techniques

DSC Analysis. A DSC 200 Phox (Netzsch Gerätebau) was used for differential scanning calorimetry (DSC) analyses.

Grazing incidence X-ray Powder Diffraction (GIXRD). GIXRD patterns were obtained at ambient temperature (25±2°C) using a Panalytical Empyrean diffractometer with CuK α radiation (λ = 1.5418 Å, 40 kV, 40 mA) and a fixed angle of incidence of 1°. The films were investigated in the range of 5 to 90° 2 θ with a step size of 0.05° 2 θ .

SEM Analysis. Scanning electron microscopy (SEM) was performed with a Jeol JSM 6510 electron microscope equipped with an energy-dispersive X-ray spectroscopy (EDX) device (Bruker Quantax 400) as well as with an ESEM Quanta 400 FEG.

References

- [1] D. Wright, *Nature* **1958**, *181*, 834.
- [2] Z. Wang, J.E. Alaniz, W. Jang, J.E. Garay, C. Dames, *Nano Lett.* **2011**, *11*, 2206.
- [3] a) D.M. Rowe, *CRC Handbook of Thermoelectrics*, CRC Press, Boca Raton, FL, **1995**; b) J.R. Drabble, C.H.L. Goodman, *J. Phys. Chem. Solids* **1958**, *5*, 142

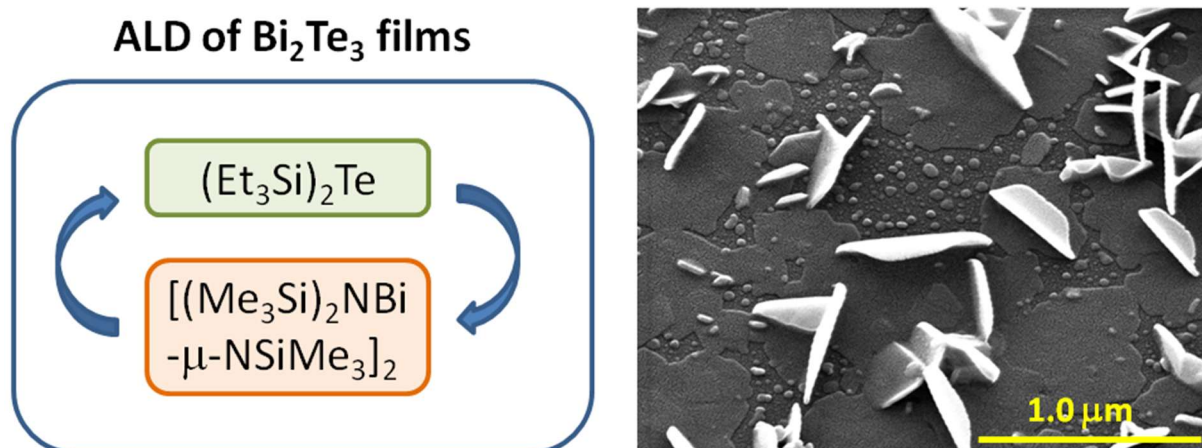
- [4] a) H. Zhang, C.-X. Liu, X.-L. Qi, X. Dai, Z. Fang, S.-C. Zhang, *Nat. Phys.* **2009**, *5*, 438; b) Y.L. Chen, J.G. Analytis, J.-H. Chu, Z.K. Liu, S.-K. Mo, X.L. Qi, H.J. Zhang, D.H. Lu, X. Dai, Z. Fang, *Science* **2009**, *325*, 178; c) D. Hsieh, Y. Xia, D. Qian, L. Wray, F. Meier, J.H. Dil, J. Osterwalder, L. Patthey, A.V. Fedorov, H. Lin, *Phys. Rev. Lett.* **2009**, *103*, 146401
- [5] a) J.E. Moore, *Nature* **2010**, *464*, 194; b) X.-L. Qi, S.-C. Zhang, *Rev. Mod. Phys.* **2011**, *83*, 1057.
- [6] a) M. Scheele, N. Oeschler, I. Veremchuk, K.-G. Reinsberg, A.-M. Kreuziger, A. Kornowski, J. Broekaert, C. Klinke, H. Weller, *ACS Nano* **2010**, *4*, 4283; b) V. Stavila, D.B. Robinson, M.A. Hekmaty, R. Nishimoto, D.L. Medlin, S. Zhu, T. M. Tritt, P.A. Sharma, *ACS Appl. Mater. Interfaces* **2013**, *5*, 6678; c) L. Chen, Q. Zhao, X. Ruan, *Mater. Lett.* **2012**, *82*, 112; d) R.J. Mehta, Y. Zhang, C. Karthik, B. Singh, R.W. Siegel, T. Borca-Tasciuc, G. Ramanath, *Nat. Mater.* **2012**, *11*, 233; e) E.E. Foos, R.M. Stroud, A.D. Berry, *Nano Letters* **2001**, *1*, 693.
- [7] a) G. Bendt, A. Weber, S. Heimann, W. Assenmacher, O. Prymak, S. Schulz, *Dalton Trans.* **2015**, *44*, 14272; b) M. Loor, G. Bendt, U. Hagemann, C. Wölper, W. Assenmacher, S. Schulz, *Dalton Trans.* **2016**, *45*, 15326; c) J. Schaumann, M. Loor, D. Ünal, A. Mudring, S. Heimann, U. Hagemann, S. Schulz, F. Maculewicz, G. Schierning, *Dalton Trans.* **2017**, *46*, 656; d) M. Loor, G. Bendt, J. Schaumann, U. Hagemann, M. Heidelmann, Christoph Wölper, S. Schulz, *Z. Anorg. Allg. Chem.* **2017**, *643*, 60.
- [8] a) V. Pore, T. Hatanpää, M. Ritala, M. Leskelä, *J. Am. Chem. Soc.* **2009**, *131*, 3478; b) M. Leskelä, V. Pore, T. Hatanpää, M. Heikkilä, M. Ritala, A. Schrott, S. Raoux, S. Rosnagel, *ECS Trans.* **2009**, *25*, 399; c) K. Knapas, T. Hatanpää, M. Ritala, M. Leskelä, *Chem. Mater.* **2010**, *22*, 1386; d) V. Pore, K. Knapas, T. Hatanpää, T. Sarnet, M. Kemell, M. Ritala, M. Leskelä, K. Mizohata, *Chem. Mater.* **2011**, *23*, 247; e) S. Zastrow, J. Gooth, T. Boehnert, S. Heiderich, W. Toellner, S. Heimann, S. Schulz, K. Nielsch, *Semicond. Sci. Technol.* **2013**, *28*, 035010; f) C. Bae, T. Bohnert, J. Gooth, S. Lim, S. Lee, H. Kim, S. Heimann, S. Schulz, H. Shin, K. Nielsch, *Semicond. Sci. Technol.* **2014**, *29*, 064003; g) D. Nminibapiel, K. Zhang, M. Tangirala, H. Baumgart, V.S.K. Chakravadhanula, C. Kübel, V. Kochergin, *ECS J. Solid State Sci. Technol.* **2014**, *3*, P95; h) T. Sarnet, T. Hatanpa, E. Puukilainen, M. Mattinen, M. Vehkamäki, K. Mizohata, M. Ritala, M. Leskela, *J. Phys. Chem. A* **2015**, *119*, 2298.
- [9] T. Sarnet, T. Hatanpää, M. Vehkamäki, T. Flyktman, J. Ahopelto, K. Mizohata, M. Ritala, M. Leskelä, *J. Mater. Chem. C* **2015**, *3*, 4820.
- [10] M. Vehkamäki, T. Hatanpää, M. Ritala, M. Leskelä, *J. Mater. Chem.* **2004**, *14*, 3191.
- [11] a) K. Moedritzer, *Inorg. Chem.* **1964**, *3*, 609; b) F. Ando, T. Hayashi, K. Ohashi, J. Koketau, *J. Inorg. Nucl. Chem.* **1975**, *37*, 2011.

- [12] a) T.J. Groshens, R.W.J. Gedridge, C.K. Lowe-Ma, *Chem. Mater.* **1994**, *6*, 727; b) T. Groshens, R. Gedridge, R. Scheri, T. Cole, in *Fifteenth International Conference on Thermoelectrics Proceedings ICT '96*, IEEE, **1996**, 430.
- [13] a) M. Leskelä, M. Ritala, *Thin Solid Films* **2002**, *409*, 138; b) M. Ritala, M. Leskelä, in *Handbook of Thin Film Materials*; H. S. Nalwa (Ed.) Academic Press: San Diego, CA, **2002**, Vol. 1, 103; c) M. Leskelä, M. Ritala, *Angew. Chem.* **2003**, *115*, 5706; *Angew. Chem. Int. Ed.* **2003**, *42*, 5548; d) M. Ritala, J. Niinistö, *ECS Trans.* **2009**, *25*, 641; e) M. Knez, K. Nielsch, L. Niinistö, *Adv. Mater.* **2007**, *19*, 3425.
- [14] a) H. Schumann, J. Kaufmann, S. Dechert, H.-G. Schmalz, *Tetrahedron Lett.* **2002**, *43*, 3507; b) C.J. Carmalt, N.A. Compton, R.J. Errington, G.A. Fisher, I. Moenandar, N.C. Norman, *Inorg. Syntheses* **1997**, *31*, 98.
- [15] W.J. Evans, D.B. Rego, J.W. Ziller, *Inorg. Chim. Acta* **2007**, *360*, 1349.
- [16] C. Hering-Junghans, A. Schulz, M. Thomas, A. Villinger, *Dalton Trans.* **2016**, *45*, 6053.
- [17] Single ALD deposition experiments (5000 pulses) with precursors **2**, **3** and **5** on Si(100) substrates at 120 °C also only showed the formation of randomly oriented, polycrystalline Bi₂Te₃ films.
- [18] a) D. Nminibapiel, K. Zhang, M. Tangirala, H. Baumgart, V.S.K. Chakravadhanula, C. Kübel, V. Kochergin, *ECS Solid State Sci. Technol.* **2014**, *3*, P95
- [19] a) G. Bendt, S. Zastrow, K. Nielsch, P.S. Mandal, J. Sánchez-Barriga, O. Rader, S. Schulz, *J. Mater. Chem. A* **2014**, *2*, 8215; b) S. Schulz, G. Bendt, J. Sonntag, A. Lorke, U. Hagemann, W. Assenmacher, *Semicond. Sci. Technol.* **2015**, *30*, 085021.
- [20] G. Bendt, S. Schulz, S. Zastrow, K. Nielsch, *Chem. Vap. Deposition* **2013**, *19*, 235.
- [21] T. Sarnet, V. Pore, T. Hatanpää, M. Ritala, M. Leskelä, A. Schrott, Y. Zhu, S. Raoux, H.-Y. Cheng, *J. Electrochem. Soc.* **2011**, *158*, D694.
- [22] M.R. Detty, M.D. Seidler, *J. Org. Chem.* **1982**, *47*, 1354.

Table of Content Entry

The capability of two bismuth amides and one cyclo-dibismadiazane to serve as ALD precursors for the deposition of Bi_2Te_3 thin films in reactions with $(\text{Et}_3\text{Si})_2\text{Te}$ was investigated and the role of substrate temperature and substrate material was verified. Bi_2Te_3 films were grown on on Si(100) and SiO_2 substrates at 170 °C using $[(\text{Me}_3\text{Si})_2\text{NBi}-\mu\text{-NSiMe}_3]_2$ **6** and $(\text{Et}_3\text{Si})_2\text{Te}$. The Bi_2Te_3 films were characterized by XRD, EDX, AFM and SEM.

Table of content graphic



DuEPublico

Duisburg-Essen Publications online

UNIVERSITÄT
DUISBURG
ESSEN

Offen im Denken

ub | universitäts
bibliothek

This text is made available via DuEPublico, the institutional repository of the University of Duisburg-Essen. This version may eventually differ from another version distributed by a commercial publisher.

DOI: 10.1016/j.jcrysro.2017.04.019

URN: urn:nbn:de:hbz:464-20201210-165727-7

This is the Authors Accepted Manuscript of an article published in: Journal of Crystal Growth 2017, Volume 470, Pages 128-134. The final version may be found at:
<https://doi.org/10.1016/j.jcrysro.2017.04.019>



This work may be used under a Creative Commons Attribution - NonCommercial - NoDerivatives 4.0 License (CC BY-NC-ND 4.0)